Conference paper

Shivender Yadav and Narayanaswamy Jayaraman*

Gradation control in the hydrodynamic diameters of mixed glycan-aglycan glycovesicles

https://doi.org/10.1515/pac-2023-0216

Abstract: Glycovesicles mimic synthetic cell membrane surfaces and aid to delineate intricate, weak carbohydrate–protein interactions. In this report, the dependence of the hydrodynamic diameters in relation to the molar fractions of carbohydrate moieties in the mixed polydiacetylene (PDA) glycovesicles is evaluated. The glycovesicles are constituted with diacetylene monomers of varying molar fractions of carbohydrate moieties and the hydrodynamic diameters are assessed without and with polymerization of the vesicles. A strong dependence of the hydrodynamic diameter of glycovesicles is seen as a function of the molar fractions and the nature of the sugar moiety being either mono- or disaccharide. A monotonous increase in the hydrodynamic diameters of the glycovesicles occurs with the increase in mole fractions of the sugar monomer lipids. Upon polymerization, the hydrodynamic diameters reduce for the vesicles with lower mole fractions of sugar monomer, whereas the reverse occurs for glycovesicles possessing higher mole fractions. Disaccharide glycovesicles possess higher hydrodynamic diameters than monosaccharide-containing vesicles. Ligand–lectin interactions were probed with lactose disaccharide-containing glycovesicles with tetrameric peanut agglutinin lectin, from which an increase in the hydrodynamic diameters is observed, as the mole fraction of sugar monomer is increased in the PDA-glycovesicles.

Keywords: Carbohydrates; cell surface mimics; dynamic light scattering; ICS-30; lectins; polydiacetylenes; vesicles.

Introduction

The ligand–receptor interactions mediated by carbohydrates and proteins are important in a myriad of biological processes [1]. The weak binding affinities in these interactions are overcome by the multivalent phenomenon, where multiple, simultaneous interactions increase the binding affinities manifold, over and above the statistical increase of the sugar moieties in the ligand [2–6]. Multivalent sugar-lectin interactions were studied earlier with the aid of glycopolymers [7], nanoparticles [8, 9], glycolipids [10–12], glycodendrimers [13–19] and glycovesicles [20–24]. The multivalent phenomenon is seen prominently in biological processes, where either an inhibition or activation of a process depends on the sugar densities present at the cell surface [25–29]. René Roy and co-workers designed glycodendrimers by varying carbohydrate ligands for targeting multiple bacterial strains [30]. In these studies, an increase in hydrodynamic diameter of the solution was observed when a hybrid of mannose and galactose-functionalized dendrimers were incubated with lectins. An increase in the hydrodynamic diameter in solutions occurred with the increase in dendrimer generations. Cloninger and co-workers reported mannose

Article note: A collection of invited papers based on presentations at the 30th International Carbohydrate Symposium (ICS-30), which was held in Brazil, 10–15 July 2022.

***Corresponding author: Narayanaswamy Jayaraman**, Department of Organic Chemistry, Indian Institute of Science, Bangalore 560012, India, e-mail: jayaraman@iisc.ac.in. https://orcid.org/0000-0001-5577-8053
Shivender Yadav, Department of Organic Chemistry, Indian Institute of Science, Bangalore 560012, India

coated PAMAM dendrimers by varying sugar densities on the dendrimer moiety [31]. Hemagglutination assay showed the maximum inhibition from dendrimer containing intermediate sugar valencies, when compared to glycodendrimers with higher sugar valencies. Studies of Percec and co-workers showed that the size, agglutination and morphology of the amphiphilic Janus glycodendrimers largely dependent on the proportion of the sugar moieties [32].

Polymeric polydiacetylene-based glycovesicles were used as probes in ligand–lectin interactions [33–35]. Our earlier studies showed the importance of proportion of sugar moieties in glycovesicles in in-plane and aggregative modes of ligand–lectin interactions [36, 37]. However, dependence of hydrodynamic diameter on the sugar ligand density of the vesicles before and after polymerization has hither-to not been realized. The hydrodynamic diameters critically depend on the mole fractions of the sugar ligands in mixed glycovesicles, leading to intra- and intermolecular nature of the ligand–lectin interactions. A systematic study of the effect of molar fractions of carbohydrate moieties, either a mono- or a disaccharide, on the hydrodynamic diameter of mixed glycovesicles is thus undertaken in the present study. The lectin interactions are also monitored in mixed glycovesicles, constituted with lactose disaccharide with peanut agglutinin. The studies demonstrate the gradation of hydrodynamic diameters and a strong dependence on mono- or disaccharide constitution and the mole fractions in the mixed glycovesicles in solutions.

Results and discussion

The glycovesicles are comprised of monomers bearing lipid and glycolipids. Monosaccharides D-mannopyranoside (**M-L**) and D-galactopyranoside (**G-L**) and disaccharide D-galactopyranosyl-β-D-glucopyranoside (lactose) glycolipid (**L-L**) were undertaken as the carbohydrate moieties in the glycolipids. In the present study, lipids with diacetylene functionality embedded in alkyl region are chosen. The diacetylene functionality undergoes a facile polymerization to result in polydiacetylene polymer upon UV irradiation [38, 39]. Polymerization leads to the vesicles being covalently-bound, precluding a lateral diffusion of the lipid molecules within the vesicles. Chemical structures of the glycolipids, **L-L**, **M-L, G-L** and a hydroxyethyl-linked non-sugar lipid **E-L** studied herein are shown in Fig. 1. Synthesis and characterizations of these glycolipids and lipids are given in the Supporting Information.

Aqueous solutions of the vesicles, containing the monomers in varying mole fractions, were prepared by mixing required molar equivalents of the lipids from the stock solutions, as follows: (i) pre-mixing of $CHCl_3$/MeOH solutions of the lipids; (ii) evaporation; (iii) vacuum-drying overnight; (iv) digestion in water; (v) sonication; (vi) hydration for 8 h at 4 °C and (vii) filtration (0.45 μ). The resulting unilamellar vesicle solutions were visibly clear solution and stable at room temperature for a few days, when kept under dark. The vesicle hydrodynamic

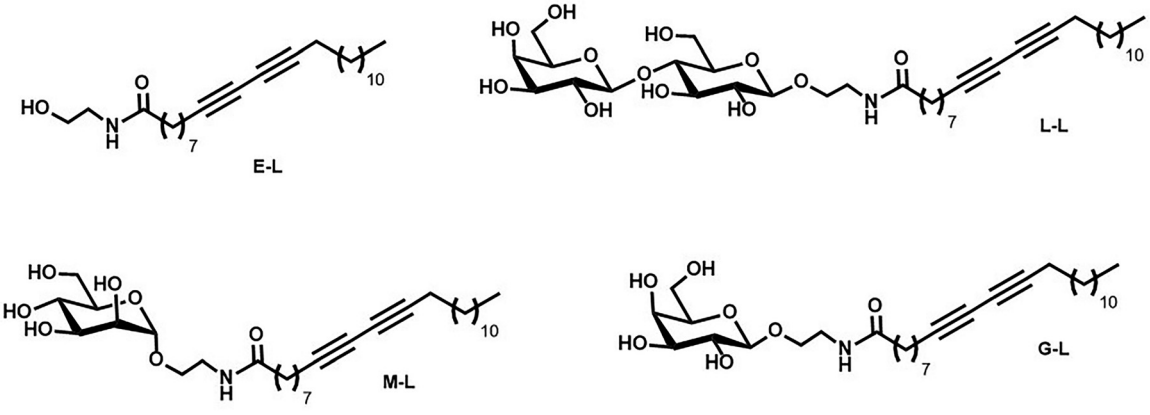

Fig. 1: Molecular structures of ethanolamine-attached diacetylene monomer **E-L** and the corresponding glycosylated monomers **L-L**, **M-L** and **G-L**.

diameters were assessed by dynamic light scattering (DLS) on the as-prepared vesicles. Figure 2 and Table 1 summarize the hydrodynamic diameter of the mixed vesicles before polymerization, prepared by varying the molar ratios of the monomer lipids. A major observation is the increase in the vesicle hydrodynamic diameter as the mole fractions of glycosylated monomer lipid increase. Monosaccharide-containing glycovesicles also exhibited a similar trend. For 10 % **M-L/E-L** mixed vesicles, the hydrodynamic diameter was 80 nm, which increased to 91 and 144 nm, when the mole fractions of the carbohydrate increased to 50 % and 100 %, respectively. In the case of **G-L/E-L** mixed vesicles, the hydrodynamic diameter increased from 63 nm to 167 nm for the 10 and 100 % mole fraction of the carbohydrate moieties in the vesicles, respectively. A comparison of 30 %, 50 % and 100 % **G-L/E-L** and **M-L/E-L**, the hydrodynamic diameter of 90, 123 and 168 nm for **G-L/E-L** was relatively higher than that for **M-L/E-L** of 83 nm, 91 nm, and 144 nm, respectively. The hydrodynamic diameter 86 nm of 10 % **L-L/E-L** vesicle increased to 108 and 111 nm when mole fraction increased to 30 % and 50 %, respectively, which increased eventually to 126 nm when the mole fraction of **L-L** increased to 80 %. These results show a gradation in the hydrodynamic diameters of the mixed glycovesicles, which depends on the constitution of the monosaccharide and the mole fractions of the glycolipid.

Exposure of the mixed glycovesicles under UV light initiates the polymerization, occurring in a few minutes and the polymer displays a deep blue solution, from the colorless un-polymerized glycovesicle solution. The polymerization requires a rigid alignment of the individual monomers, where the diacetylene moiety is within 3–4 Å and ~45° orientation in each monomer. The bilayer vesicles constituted with the monomers would possess an aq. interior [40]. Assessment of the hydrodynamic diameters of the polymerized glycovesicles across varying mole fractions show that a reduction in the case of **M-L/E-L** and **G-L/E-L** at 10 and 30 % glycovesicles. Before and after polymerization of 10 % **M-L/E-L**, the hydrodynamic diameters were 81 and 65 nm, respectively. Similar reduction was observed for 30 % **M-L/E-L** glycovesicle also. Such a reduction narrowed as the mole fraction of the sugar component increased and at 100 % **M-L** vesicle, the hydrodynamic diameter after polymerization surpassed to 186 nm, as compared to that before polymerization at 145 nm. This trend of reduction in the hydrodynamic diameters at lower mole fractions of the glycolipid and a considerable increase of the same at higher mole fractions is observed for **G-L/E-L** vesicles also. With the disaccharide **L-L/E-L** glycovesicles, a significant increase in the hydrodynamic diameters for all mole fractions of the glycolipid above 30 %. The disaccharide mixed glycovesicles, swelling of the hydrodynamic diameters occurred at the lesser mole fraction of the glycolipid, whereas such a swelling occurred at 80 and 100 % glycolipids in the case of the monosaccharide-containing glycovesicles.

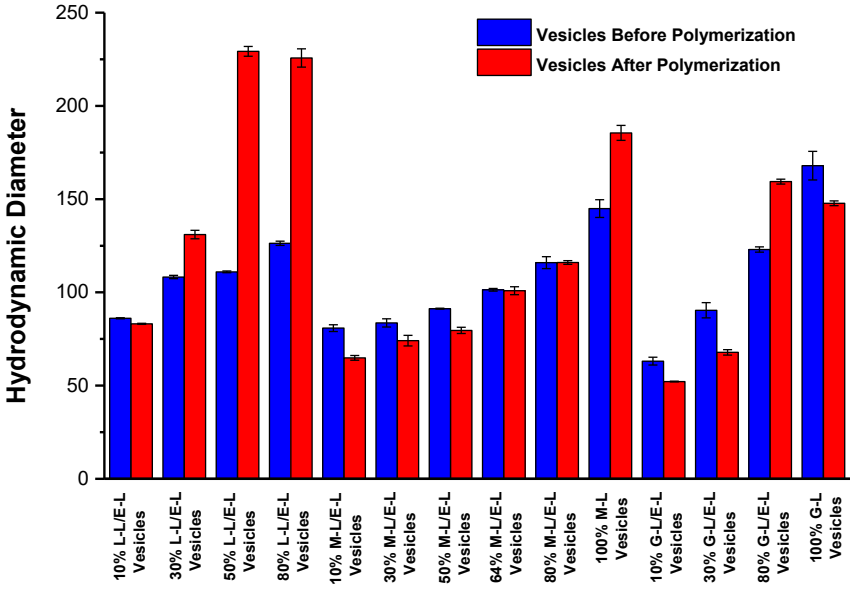

Fig. 2: Bar diagram of the hydrodynamic diameters (in nm) of mixed glycovesicles with varying mole fractions glycosyl lipid monomers **L-L**, **M-L** and **G-L** in **E-L**.

Table 1: Dependence of hydrodynamic diameters (in nm) on the mole fraction of glycolipid in mixed glycan-aglycan vesicles.

Mixed vesicles	Mole fraction of glycolipid in glycan-aglycan mixed vesicles					
	10 %	30 %	50 %	64 %	80 %	100 %
M-L/E-L[a]	80.8 ± 1.8	83.6 ± 2.1	91.2 ± 0.3	101.4 ± 0.7	115.9 ± 3.2	144.9 ± 4.7
M-L/E-L[b]	64.8 ± 1.2	74.09 ± 2.5	79.5 ± 1.6	100.8 ± 2.1	116 ± 1	185.5 ± 4.1
G-L/E-L[a]	63.1 ± 2.1	90.4 ± 4.1	–	–	123 ± 1.4	167.9 ± 7.7
G-L/E-L[b]	52.18 ± 0.2	67.83 ± 1.5	–	–	159.4 ± 1.3	147.7 ± 1.3
L-L/E-L[a]	86.1 ± 0.2	108.2 ± 0.9	110.9 ± 0.5	–	126.3 ± 1.1	–
L-L/E-L[b]	83.1 ± 0.2	130.8 ± 2.1	229.5 ± 2.6	–	225.7 ± 4.9	–

[a]Before polymerization. [b]After polymerization.

Changes to hydrodynamic diameters of the glycovesicles upon interaction with tetrameric lectin peanut agglutinin were studied with **L-L**/**E-L** glycovesicles, at 5, 30 and 60 min durations. Due to the well-defined binding site characteristics, lactose-PNA system was selected in the study [41]. The studies were conducted by the addition of the vesicle solution to a buffer solution of lectin (1 mM PBS, 10 mM NaCl, 1 mM of $CaCl_2$ and $MnCl_2$), keeping

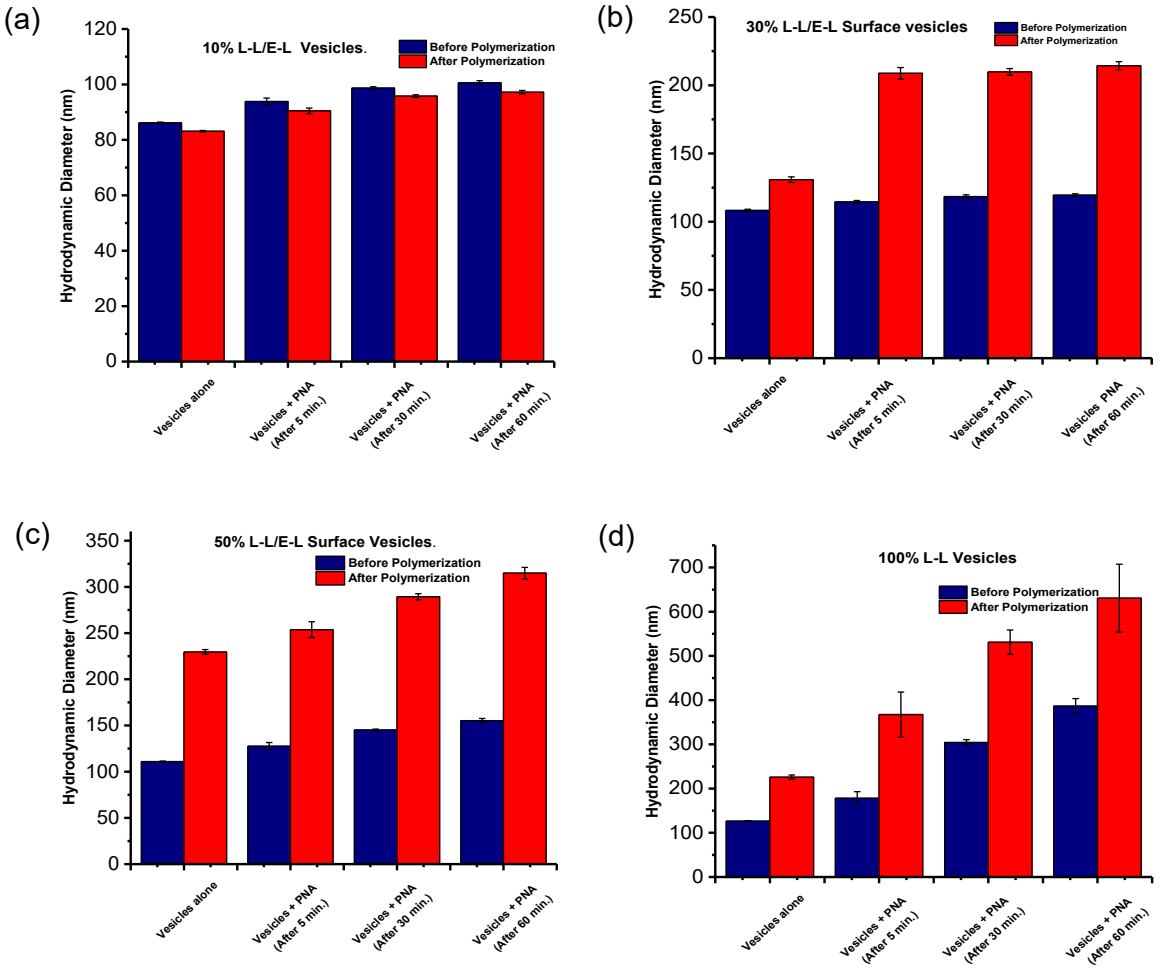

Fig. 3: Plots of the changes in the vesicle hydrodynamic diameters upon complexation with lectin PNA before (blue) and after (red) polymerization.

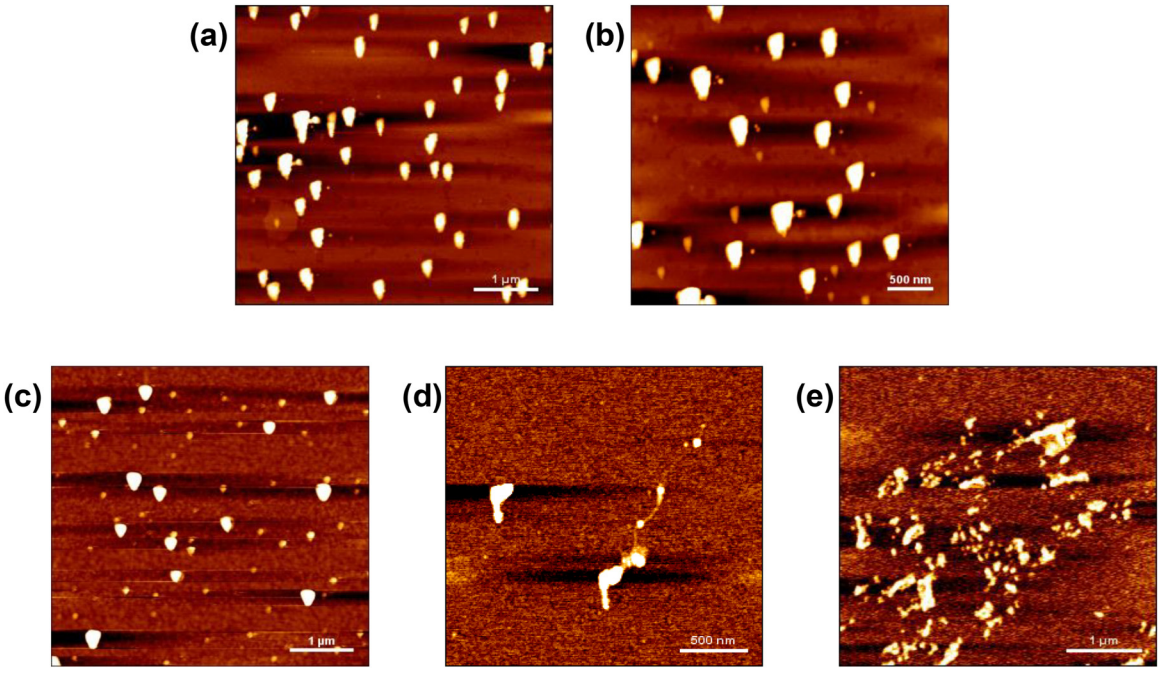

Fig. 4: AFM images of (a) 10 % **L-L/E-L** vesicle; (b) lectin complexed 10 % **L-L/E-L** vesicle; (c) 80 % **L-L/E-L** vesicle; (d) and (e) lectin complexed with 80 % **L-L/E-L** vesicle.

Table 2: Hydrodynamic diameters of the **L-L/E-L** vesicles upon interaction with PNA.

L-L/E-L	Vesicle alone	Vesicles + PNA (after 5 min)	Vesicles + PNA (after 30 min)	Vesicles + PNA (after 60 min)
10 %[a]	86.1 ± 0.2	93.8 ± 1.2	98.6 ± 0.4	100.5 ± 0.8
10 %[b]	83.1 ± 0.2	90.4 ± 1	95.7 ± 0.4	97.1 ± 0.6
30 %[a]	108.2 ± 0.9	114.5 ± 1.0	118.4 ± 1.2	119.4 ± 0.9
30 %[b]	130.8 ± 2.1	208.8 ± 4.2	209.8 ± 2.4	214.3 ± 2.9
50 %[a]	110.9 ± 0.5	127.5 ± 3.9	145.1 ± 0.9	155.2 ± 2.3
50 %[b]	229.5 ± 2.6	253.7 ± 8.5	289.3 ± 3.2	314.8 ± 6.2
80 %[a]	126.3 ± 1.1	178.1 ± 14.8	304.1 ± 6.5[c]	386.5 ± 16.8[d]
80 %[b]	225.7 ± 4.9	367.3 ± 50.8[e]	531 ± 27.5[f]	630.5 ± 76.7[g]

[a]Before polymerization. [b]After polymerization. Multi-modal distribution of particles. Hydrodynamic radius of each distribution (nm) (fractional intensities in %) are: [c]425.1 (75.3), 104.4 (17.3) and 5069 (7.4); [d]523.9 (67.1), 114.5 (19) and 4921 (13.9); [e]327 (96.5) and 5464 (3.5); [f]442.3 (86.8), 5259 (12.1) and 36.8 (1.2); [g]595 (73.2), 163.4 (22.2) and 5505 (4.6).

the lectin concentration uniform across varying mole fractions of **L-L/E-L** vesicles. The facile photo-polymerization of diacetylene moiety also permitted the ligand–receptor studies to be conducted on the covalently-bound polymeric vesicles. Figure 3 and Table 2 summarize changes in the hydrodynamic diameters of the vesicles upon interaction with the lectin.

At 10 % **L-L/E-L** vesicle, the mean hydrodynamic diameter 86.1 nm increased to 93.8 nm upon complexation with lectin, when measured after 5 min and the same increased to 100.6 nm after 60 min. No visible precipitation was observed on leaving the solution for longer time. Irradiation to UV light led to diacetylene polymerization, resulting in a violet solution (λ_{max} 636 nm) (Fig. S25). Interaction with the lectin led to insignificant increases in the hydrodynamic diameter from 90.5 nm in 5 min to 97.2 nm after 60 min. Decrease in UV absorbance was observed, with no change in λ_{max} and solution color after addition of PNA. Similarly, 30 % **L-L/E-L** did not show perceptible

increase in the hydrodynamic diameter of the vesicle upon interaction with the lectin, vesicle size increased from 108.2 nm to 120 nm, after 60 min of lectin addition. Polymerization of the diacetylene moiety afforded violet polymeric vesicles solution (Fig. S26). Upon addition of lectin, the particle size 130.8 nm of polymeric vesicles increased to 208.8 and 214.3 nm in 5 and 60 min, respectively.

For vesicles constituted with 50 % **L-L**/**E-L**, the average mean hydrodynamic diameter of vesicles alone before polymerization was 110.9 nm, which upon interaction with lectin PNA increased the size to 127.6 and 155.2 nm in 5 and 60 min, respectively. Polymerization resulted in a violet solution (Fig. S27) and the particle size 229.6 nm of polymeric vesicles increased considerably to 314.9 nm after 30 min of addition of lectin, with attendant cloudiness of the solution after several hours. In 80 % **L-L**/**E-L** vesicle solutions before polymerization, changes in the hydrodynamic diameters of the vesicles were significant, particle size of 126.3 nm increased to 304.1 and 386.5 nm, respectively, after 30 min and 1 h duration of the lectin addition. The colorless solutions turned to magenta red (λ_{max} 531.5 nm) upon polymerization. The hydrodynamic diameter of polymeric 80 % **L-L**/**E-L** vesicles (225 nm) changed drastically upon addition of the lectin to 367.3, 531 and 630.6 nm after 5 min. 30 min. and 1 h duration, respectively. A reduction in the λ_{max} absorbance intensity was also observed upon addition of lectin to polymeric vesicles. However, no change in color and shift in λ_{max} value occurred after the addition of the lectin to the polymeric vesicles solution (Fig. S28).

AFM analysis was conducted further, for which the glycovesicles were drop-casted on the fresh mica surface and analyzed by the tapping mode. For 10 % **L-L**/**E-L** glycovesicle with and without complexation appeared closely in particle size, morphology and height (Fig. 4a and b). Whereas the spherical particles of 80 % **L-L**/**E-L** vesicle turns into large, irregular particle heights and sizes of varying dimensions, leading up to micron sizes upon complexation with the PNA (Fig. 4c–e).

The hydrodynamic diameters of the vesicles-lectin complexes increased with the increase in the percentage mole fractions and durations of the glycovesicles-lectin complexes. Further, the particle sizes were higher for polymeric vesicles, as compared to un-polymerized vesicles after the addition of the lectin in solution.

Complexation of **M-L**/**E-L** glycovesicles with PNA did not lead to perceptible increases in the hydrodynamic diameter, either before or after polymerization (Fig. 5), indicating the requirement of specificity in the sugar-lectin interaction, as in the case of **L-L**/**E-L** glycovesicles with PNA.

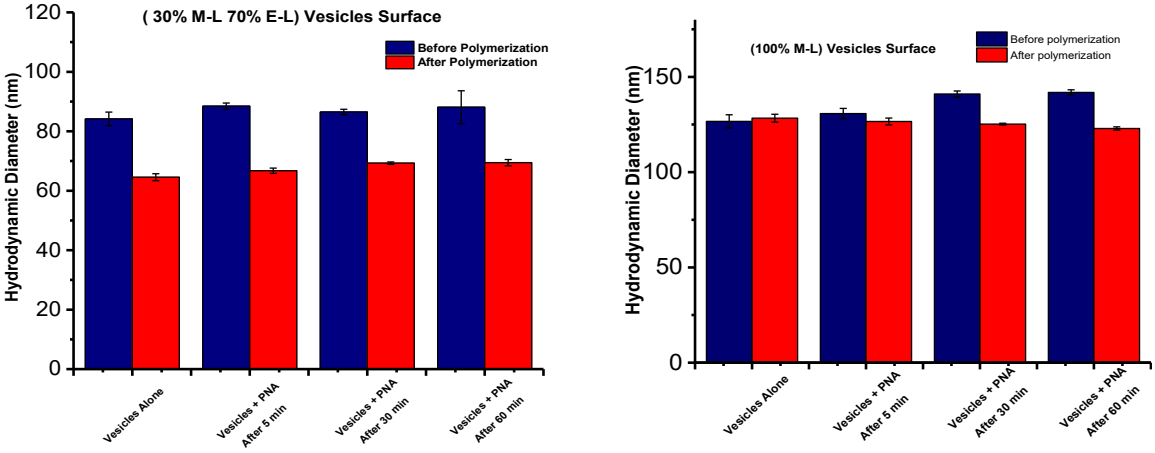

Fig. 5: Plots of the changes in the 30 % and 100 % **M-L**/**E-L** vesicle hydrodynamic diameters upon complexation with PNA (before and after polymerization).

Conclusions

The studies herein demonstrate the key effects of carbohydrate moieties on the glycovesicles hydrodynamic diameters. A gradation in the hydrodynamic diameter of the glycovesicles is observed depending on the mole fraction of glycolipid and the nature of the carbohydrate moiety. For monosaccharide glycovesicles, there was a reduction in the hydrodynamic diameters up to 50 % of **M-L**/**E-L** and **G-L**/**E-L**, followed by an increase at the 80 % and 100 % ratios. Such a reduction did not occur for the disaccharide, monotonous increase of the hydrodynamic diameter occurred from 30 % **L-L** in **E-L**. Further, polymeric glycovesicles showed higher hydrodynamic diameters, as compared to unpolymerized vesicles after the addition of the lectin in the ligand–lectin complexations. The observations of the present study have a significance in the continuing efforts to understand the effect of the extent of glycan functionalization on the hydrodynamic diameters of the glycovesicles and the interactions of glycovesicles with lectins.

Supporting information

Supporting information can be accessed online for free. This section includes NMR spectra of **G-L** and **L-L**, DLS data and UV–Vis spectra.

Acknowledgements: SY is grateful to research fellowship of the Indian Institute of Science, Bangalore, India.
Research funding: We are grateful to SERB (CRG/2022/007786), DST, New Delhi for a financial support of this work.

References

[1] A. Imberty, A. Varrot. *Curr. Opin. Struct. Biol.* **18**, 567 (2008).
[2] L. L. Kiessling, J. E. Gestwicki, L. E. Strong. *Angew. Chem. Int. Ed.* **45**, 2348 (2006).
[3] T. K. Dam, C. F. Brewer. *Adv. Carbohydr. Chem. Biochem.* **63**, 139 (2010).
[4] N. Jayaraman. *Chem. Soc. Rev.* **38**, 3463 (2009).
[5] R. J. Pieters. *Org. Biomol. Chem.* **7**, 2013 (2009).
[6] N. Jayaraman, K. Maiti, K. Naresh. *Chem. Soc. Rev.* **42**, 4640 (2013).
[7] Y. M. Chabre, R. Roy. *Adv. Carbohydr. Chem. Biochem.* **63**, 165 (2010).
[8] S. Takae, Y. Akiyama, H. Otsuka, T. Nakamura, Y. Nagasaki, K. Kataoka. *Biomacromolecules* **6**, 818 (2005).
[9] X. Wang, O. Ramström, M. Yan. *Anal. Chem.* **82**, 9082 (2010).
[10] B. N. Murthy, N. H. Voelcker, N. Jayaraman. *Glycobiology* **16**, 822 (2016).
[11] N. M. Bandaru, S. Sampath, N. Jayaraman. *Langmuir* **21**, 9591 (2005).
[12] C. S. Altamirano, S. A. Sanchez, N. F. Ferreyra, G. Gunther. *Colloids Surf. B: Biointerfaces* **158**, 539 (2017).
[13] E. K. Woller, E. D. Walter, J. R. Morgan, D. J. Singel, M. J. Cloninger. *J. Am. Chem. Soc.* **125**, 8820 (2003).
[14] T. Fukuda. *Polym. J.* **51**, 535 (2019).
[15] E. M. Munoz, J. Correa, R. Riguera, E. F. Megia. *J. Am. Chem. Soc.* **135**, 5966 (2013).
[16] S. P. Bernhard, M. S. Fricke, R. Haag, M. J. Cloninger. *Polym. Chem.* **11**, 3849 (2020).
[17] M. L. Wolfenden, M. J. Cloninger. *Bioconjugate Chem.* **17**, 958 (2006).
[18] Y. M. Chabre, A. Papadopoulos, A. A. Arnold, R. Roy. *Beilstein J. Org. Chem.* **10**, 1524 (2014).
[19] Y. M. Chabre, R. Roy. *Chem. Soc. Rev.* **42**, 4657 (2013).
[20] G. B. Thomas, L. H. Rader, J. Park, L. Abezgauz, D. Danino, P. De Shong, D. S. English. *J. Am. Chem. Soc.* **131**, 5471 (2009).
[21] R. Sundler. *Fed. Eur. Biochem. Soc.* **141**, 11 (1982).
[22] A. Mauceri, A. Fracassi, M. D'Abramo, S. Borocci, L. Giansanti, A. Piozzi, L. Galantini, A. Martino, V. D'Aiuto, G. Mancini. *Colloids Surf. B: Biointerfaces* **136**, 232 (2015).
[23] B.-S. Kim, D.-J. Hong, J. Bae, M. Lee. *J. Am. Chem. Soc.* **127**, 16333 (2005).
[24] G. J. L. Bernardes, R. Kikkeri, M. Maglinao, P. Laurino, M. Collot, S. Y. Hong, B. Lepenies, P. H. Seeberger. *Org. Biomol. Chem.* **8**, 4987 (2010).
[25] R. A. Mariuzza, W. Held. *Cell. Mol. Life Sci.* **68**, 3469 (2011).
[26] C. D. Rillahan, M. S. Macauley, E. Schwartz, Y. He, R. McBride, B. M. Arlian, J. Rangarajan, V. V. Fokin, J. C. Paulson. *Chem. Sci.* **5**, 2398 (2014).
[27] L. S. Chang, R. T. O'Donnell, J. M. Tuscano. *BioDrugs* **27**, 293 (2013).

[28] S. Mesch, K. Lemme, M. Wittwer, H. Koliwer-Brandl, O. Schwardt, S. Kelm, B. Ernst. *ChemMedChem* **7**, 134 (2012).
[29] P. R. Crocker, J. C. Paulson, A. Varki. *Nat. Rev. Immunol.* **7**, 255 (2007).
[30] C. Sehad, T. C. Shiao, L. M. Sallam, A. Azzouz, R. Roy. *Molecules* **23**, 1890 (2018).
[31] E. K. Woller, E. D. Walter, J. R. Morgan, D. J. Singel, M. J. Cloninger. *J. Am. Chem. Soc.* **125**, 8820 (2003).
[32] Q. Xiao, S. Zhang, Z. Wang, S. E. Sherman, R.-O. Moussodia, M. Peterca, A. Muncan, D. R. Williams, D. A. Hammer, S. Vértesy, S. André, H.-J. Gabius, M. L. Klein, V. Percec. *Proc. Natl. Acad. Sci. U.S.A.* **113**, 1162 (2016).
[33] D. H. Charych, J. O. Nagy, W. Spevak, M. D. Bednarski. *Science* **261**, 585 (1993).
[34] M. van den Heuvel, D. W. P. M. Löwik, J. C. M. van Hest. *Biomacromolecules* **11**, 1676 (2010).
[35] Y. Singh, N. Jayaraman. *Macromol. Chem. Phys.* **218**, 1 (2017).
[36] S. Yadav, K. Naresh, N. Jayaraman. *ChemBioChem* **22**, 485 (2021).
[37] S. Yadav, K. Naresh, N. Jayaraman. *ChemBioChem* **22**, 3075 (2021).
[38] G. Z. Wegner. *Z. Naturforsch. B* **24**, 824 (1969).
[39] J.-S. Filhol, J. Deschamps, S. G. Dutremez, B. Boury, T. Barisien, L. Legrand, M. Schott. *J. Am. Chem. Soc.* **131**, 6976 (2009).
[40] C. X. Guo, P. Boullanger, T. Liu, L. Jiang. *J. Phys. Chem. B* **109**, 18765 (2005).
[41] V. J. Pratap, G. M. Bradbrook, G. B. Reddy, A. Surolia, J. Raftery, J. R. Helliwell, M. Vijayan. *Acta Crystallogr.* **D57**, 1584 (2001).

Supplementary Material: This article contains supplementary material (https://doi.org/10.1515/pac-2023-0216).